

Deciphering the 3D Orion Nebula-IV: The HH 269 Flow Emerges from the Orion-S Embedded Molecular Cloud

C. R. O'Dell , N. P. Abel , and G. J. Ferland

Department of Physics and Astronomy, Vanderbilt University, Nashville, TN 37235-1807, USA

MCGP Department, University of Cincinnati, Clermont College, Batavia, OH, 45103, USA

Department of Physics and Astronomy, University of Kentucky, Lexington, KY 40506, USA

Received 2021 January 12; revised 2021 January 28; accepted 2021 January 30; published 2021 March 10

Abstract

We have extended the membership and determined the 3D structure of the large (0.19 pc) HH 269 sequence of shocks in the Orion Nebula. All of the components lie along a track that is highly tilted to the plane of the sky and emerge from within the Orion-S embedded molecular cloud. Their source is probably either the highly obscured mm 9 source associated with a high N_2H^+ density core (more likely) or the more distant star COUP 632 (less likely). The former must be located in the photon dominated region (PDR) underlying the ionized surface of the Orion-S Cloud, while the latter would be embedded within the Orion-S Cloud. The flows seem to be episodic, with intervals of 1900–2600 yr or 700–2600 yr if COUP 632 is the source.

Unified Astronomy Thesaurus concepts: Herbig-Haro objects (722); H II regions (694)

1. Introduction

This paper is the fourth in a series reporting on the properties of features within the Orion Nebula. Paper I (O'Dell et al. 2020) dealt with large-scale features, especially the foreground layer of ionized material, the placement of the embedded Orion-S Molecular Cloud (henceforth Orion-S Cloud), and the more distant overlying ionized layer designated as the nearer ionized layer (NIL). Paper II (O'Dell et al. 2021a) identified a new major feature of the nebula lying ESE-WNW across the nebula and with the Orion-S Cloud on its northern boundary. These first two papers used spectra averaged over blocks of 10" ×10" (velocity resolution of 10 km s⁻¹). Paper III (O'Dell et al. 2021b) used several fullspatial-resolution (about 2") sequences of spectra, denoted therein as "profiles", to determine the properties of the brightest part of the Orion Nebula, which occurs at the NE boundary of the Orion-S Cloud. In that study, a central 30'' diameter region designated the "Crossing" was spectroscopically very complex and informed the spatial structure of the photoionized layer of the Orion-S Cloud that faces the observer. These three papers give summaries of our preceding knowledge of the structure of the Huygens Region (the bright central portion of the Orion Nebula) and the progressive improvement of this knowledge.

From a star formation point of view, the arguably most interesting region identified in Papers I–III is the Orion-S Cloud. These earlier papers established that this feature is a host for young stars, many of which have collimated outflows. The study of these outflows requires using images and spectra in a different manner. The most important procedural differences are that in the present study we draw on time-lapse images made with the Hubble Space Telescope to identify high-velocity flows associated with HH 269 and that we employ high-spatial-resolution radial velocities of these features to determine their 3D locations and motions. This then allows us to precisely constrain the location of the source driving these outflows.

The nomenclature for velocity and groupings of data in the present study are the same as in Paper III. Radial velocities are given in ${\rm km\,s}^{-1}$ in the heliocentric system. ⁴ The observational

material used here is described in Section 2. The importance of the motions in the Crossing is explained in Section 3, while the new properties of the HH 269 flow are described in Section 4. The 3D positions and motions of the HH 269 Groups are presented in Section 4.2 and their origin is presented in Section 5. A nearby un-aligned series of shocks is described in Section 6. The episodic nature of the HH 269 flow is discussed in Section 7. The results of this study are related to those provided in the earlier papers in this series in Section 8.

2. Observations

The spectroscopic data we use in this study are the same as in Paper III, and we have made even more extensive use of archival Hubble Space Telescope (HST) images. Again, we draw on the high-spectral-resolution "Spectroscopic Atlas of Orion Spectra" of García-Díaz et al. (2008), compiled from a series of north–south slit spectra at intervals of $2^{\prime\prime}$ and a velocity resolution of $10~{\rm km\,s^{-1}}$.

3. The Important Role of the Orion-S Crossing

The Orion-S Crossing (henceforth, the Crossing) is a 30" diameter region centered at 5:35:13.95–5:23:49.2 In Papers II and III we established that this is the region of origin of changes in the foreground NIL and the ionized surface of the Orion-S embedded molecular cloud. It is a high (closer to the observer) region on the NE edge of the Orion-S Cloud.

Within the Crossing we define the Core as the region where the three Profiles discussed in Paper III show that the signals from the $V_{\rm long,[O~III]}$ ([O III] 500.7 nm emission) and $V_{\rm short,[O~III]}$ emission abruptly become comparable. The former is a longer wavelength component of the deconvolved line profile that is usually identified with the main ionization front (MIF) while the latter is a shorter wavelength component usually identified with foreground lower velocity material. This common region is outlined in red in Figure 1. The Core agrees in position with the areas in Paper III where we found that the signal ratios ($S_{\rm short,[O~III]}/S_{\rm long,[O~III]}$) are anomalously strong, usually from the MIF.

⁴ Conversion to local standard of rest is done by subtracting 18.1 km s⁻¹.

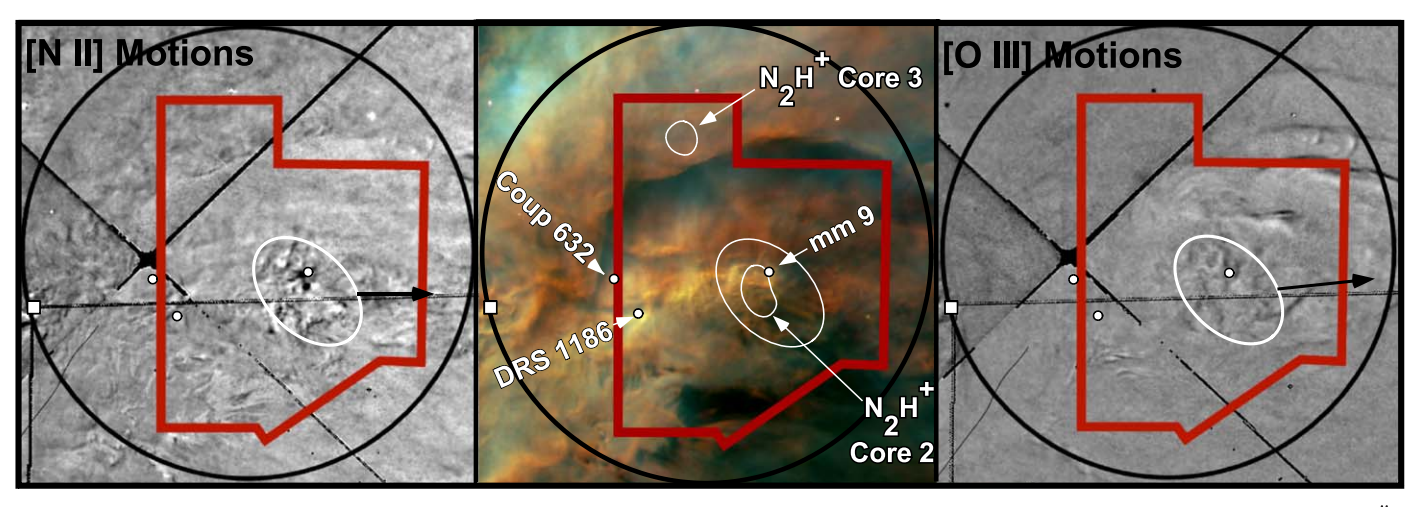


Figure 1. Three $30'' \times 30''$ panels centered on the Crossing (the large black circle). The central panel is made from HST camera WFC3 images with a scale of 0.''04 pixels (HST program GO 12543, (O'Dell et al. 2015)). The color coding is Red-[N II], Green-Hα, and Blue-[O III]. The other panels depict motions, the left in [N II] and the right in [O III]. These latter are the ratio of early over late images, and so motion is indicated by the dark edge outside of a bright edge as described in O'Dell et al. (2015). The red line gives the boundaries of the Core, where the $V_{\text{low,[O III]}}$ and $V_{\text{long,[O III]}}$ signals are comparable. The long thin black lines are artifacts at the edges of the earlier images. The three small filled circles are at the positions of the compact sources within the Crossing that lie near the central axis of the HH 269 flow. The white ellipse encloses the features for which tangential motions could be determined (the Crossing-Group). The black arrows indicate the average tangential velocities for the group (from Table 1 for both [N II] ($V_{\text{tan,[N II]}} = 25 \pm 12 \text{ km s}^{-1}$, PA = 270° ± 10°) and [O III] ($V_{\text{tan,[O III]}} = 32 \pm 12 \text{ km s}^{-1}$, PA = 276° ± 35°). The irregular white lines designate the central contours of the N₂H⁺ Cores 2 (south) and 3 (north) from Teng & Hirano (2020), Section 5.1.1. The square indicates the position from which the HH 1132 east-jet emerges, as discussed in Section 5.1.

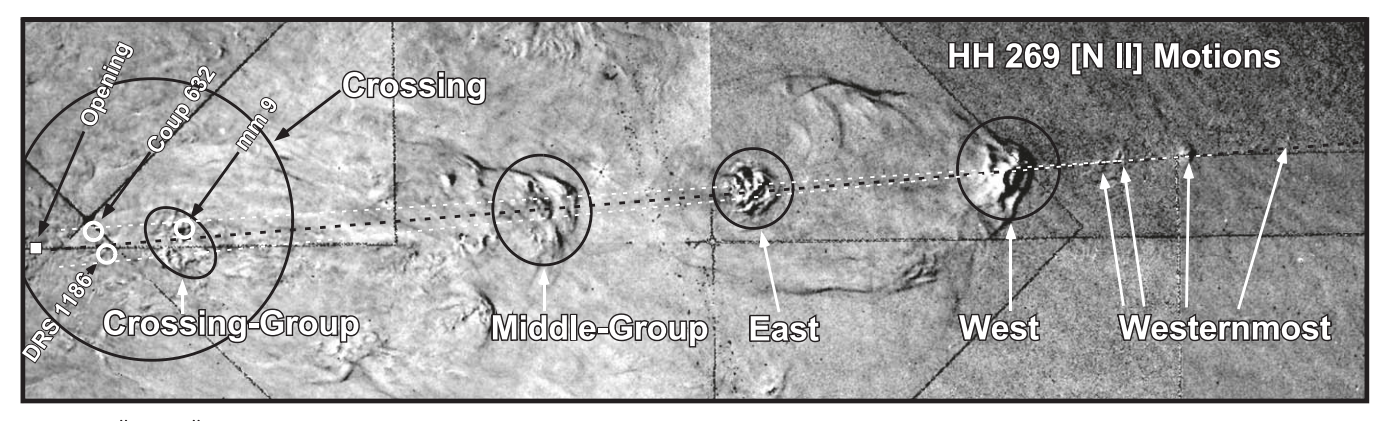


Figure 2. $143.''2 \times 40.''6$ F658N [N II] motions image centered at 5:35:10.0-5:23:50 showing the east and west components of HH 269 designated in Bally et al. (2000), the westernmost components designated in O'Dell et al. (2015), the Middle-Group components studied in O'Dell et al. (2015) which we now designate as part of the HH 269 system, and the Crossing-Group component highlighted in this study. The dashed black line indicates the common axis of the components at $PA = 275^{\circ}$ and the dashed white lines $\pm 1^{\circ}$ uncertainty in that value. The H_2 knot 2–4 (Stanke et al. 2002) lies 91'' at $PA = 277^{\circ}$ from the westernmost marked component. The positions of COUP 632, DRS 1186, and mm 9 are shown as open circles and the filled white square indicates the position from which the east-moving HH 1132 east-jet emerges, as discussed in Section 5.1. The large circle on the east end indicates the Crossing from Figure 1.

 Table 1

 Tangential and Radial Velocities of HH 269 Components^a

Group	$V_{ m tan,[N~II]}$	PA _[N II]	$V_{ m [N~II]}$	V _{tan,[O III]}	PA _[O III]	$V_{ m [O~III]}$
Crossing-Group	25 ± 12	270 ± 10	-11 ± 3	32 ± 12	276 ± 35	-30 ± 3
Middle-Group ^b	31 ± 11	273 ± 16	-9 ± 3	36 ± 19	262 ± 14	-40 ± 1
East ^c	42 ± 9	277 ± 13	-13 ± 1			
West	73 ± 16	270 ± 11	-23 ± 2	52 ± 19	288 ± 7	-17 ± 3

Notes

Within the Core we find blueshifted components not found in nearby spectra. Their velocities are given in Table 1 along with velocities from HH 269 features identified in Figure 2. As the spectra were relatively wide, the locations of these components are most likely to be in the central region covered by the three profiles. This region was included in the tangential

^a Position angles (PAs) in ° are from O'Dell et al. (2015) except where measured in this study and tangential velocities are calculated using an assumed distance of 388 pc (Kounkel et al. 2017). The positions of nonCrossing Groups are indicated in Figure 2 and are given in Table 3.

^b $V_{\rm [N~II]}$ is from Large Sample 80, -30 in Paper II.

^c $V_{\text{[N II]}}$ is from Walter et al. (1995).

Table 2
HH 269 Components 3D Velocities and Angles

Designation	Line	$V_{\mathrm{3D}}^{\mathrm{a}}$	$\Theta^{\mathbf{a}}$
Crossing-Group	[N II]	69 ± 12	$57^{\circ} \pm 7^{\circ}$
"	[O III]	65 ± 12	$61^{\circ} \pm 9^{\circ}$
Middle-Group	[N II]	46 ± 12	$49^{\circ} \pm 10^{\circ}$
"	[O III]	76 ± 20	$62^{\circ} \pm 11^{\circ}$
East	[N II]	58 ± 10	$44^{\circ} \pm 6^{\circ}$
West	[N II]	88 ± 15	$34^{\circ}\pm6^{\circ}$
"	[O III]	68 ± 20	$40^{\circ}\pm14^{\circ}$
Average	[N II] and [O III]	66 ± 14	$48^{\circ}\pm10^{\circ}$

Note.

^a V_{3D} is the spatial velocity of the Group in km s⁻¹, Θ is the angle of the velocity vector out of the plane of the sky and toward the observer. The assumed radial velocity of the Orion-S Cloud was 27 km s⁻¹. The average was calculated giving triple weight to the much more numerous [N II] motions.

velocity study of O'Dell et al. (2015), which found multiple high tangential features. The outer panels of Figure 1 show two tangential velocity motion images (first epoch image over second epoch image). The light-line ellipse encloses the region where moving objects were found (seven in [N II] and two in [O III]).

Three compact sources in the Crossing and lying near the axis of HH 269 are shown in all panels of Figure 1: COUP 632Getman et al. (2005) (5:35:14.40-5:23:50.9), DRS 1186Da Rio et al. (2009) (5:35:14.29-5:23:53.1), and mm 9Eisner & Carpenter (2006) (5:35:13.72-5:23:50.6).

Using both the average radial and tangential velocities we calculated the spatial motions presented in Table 2. The high-velocity features arising from the Crossing are moving at about 65 km s⁻¹ at an angle $\Theta \simeq 60^{\circ}$ from the plane of the sky (toward the observer) toward position angle (PA) $\simeq 276^{\circ}$.

4. Properties of the HH 269 Series of Shocks

The series of features associated with HH 269 are among the largest structures within the Huygens Region. Their two brightest components were first studied in detail by Walter et al. (1995) and subsequently designated as HH 269-East and HH 269-West (Bally et al. 2000 ; henceforth, East and West in this study). The $\rm H_2$ study of Stanke et al. (2002) covered the full Extended Orion Nebula (EON) and O'Dell et al. (2015) assigned Stanke's more distant feature 2–4 as part of HH 269 on the basis of its orientation along the axis of the east—west features. O'Dell et al. (2015) added multiple small moving features to the west of the West component.

4.1. Two New Components of HH 269

We now add two groupings of shocks (the Middle-Group and the Crossing-Group) to extend the series of components to the east (the latter addition was suggested in O'Dell et al. (2015)), as shown in Figure 2. A major feature within the Crossing is the low-ionization "squiggly" feature called the West-Jet in O'Dell et al. (2015). In Paper III we established that the West-Jet name is not a good description because only the west end of it has a detectable motion, while a [N II] bright feature at 5:35:13.90–5:23:52 is the highly tilted side of a stationary escarpment facing north. The latter feature is called the Ledge in Paper III and all of the West-Jet is now called the Extended-Ledge, which is a mix of moving and stationary

Table 3 Positions^a of HH 269 Components

Designation	R.A.	Decl.
Crossing-Group	5:35:13.71	-5:23:52
Middle-Group	5:35:11.08	-5:23:49
East	5:35:09.65	-5:23:47
West	5:35:07.77	-5:23:46
Westernmost	5:35:07.12	-5:23:44
Westernmost	5:35:06.98	-5:23:43
Westernmost	5:35:06.46	-5:23:43
Westernmost	5:35:05.75	-5:23:41
Stanke 2–4	5:34:59.8	-5:23:30

Note.

Table 43D Positions of HH 269 Components

Component	Δ Tangential ^a	Adopted ⊖	$\Delta D^{\mathbf{a}}$
Crossing-Group	0.0	59°	0
Middle-Group	0.065	56°	-0.11
East	0.105	44°	-0.17
West	0.157	•••	-0.22

Note.

^a Distances are in pc relative to the Crossing-Group in the plane of the sky (Δ Tangential) and along the line of sight (Δ D, where negative numbers are toward the observer).

features. All of these lie along an axis of $PA = 275^{\circ}$. The observed and derived characteristics of the components are presented in Tables 1–3.

4.2. 3D Positions of the HH 269 Components

 $V_{\rm tan}$ (motion in the plane of the sky) and $V_{\rm r}$ (radial velocity) have been determined for the sequence of HH 269 components Crossing-Group–Middle-Group–East–West (Table 1). This allows the calculation of the spatial velocity ($V_{\rm 3D}$) and the angle (Θ) with respect to the plane of the sky with the results shown in Table 2. Having the separations in the plane of the sky (Table 3) and the velocity vectors, one can calculate the relative positions along the line of sight. Using these results we calculated the positions of each component with respect to the Crossing-Group (Table 4), where we see that the HH 269 sequence is highly tilted with respect to the plane of the sky.

We conclude that the Crossing is where the axis of the HH 269 sequence emerges from behind the surface of the Orion-S Cloud. The source of the components must be at or east of the Crossing-Group.

5. Origin of the HH 269 Components

Two basic approaches are used to determine the location of the source of the HH 269 sequence, proximity to the axis of the HH 269 components, and locations suggested by $V_{\rm 3D}$. We see below that these suggest two likely sources.

5.1. Origin from Positions and Directions

The dashed black line with $PA=275^{\circ}$ in Figure 2 shows that the axis of the HH 269 components pass near three compact sources (from the west mm 9, DRS 1186, and COUP 632)

a 2000.0

within the Dark Arc (the dark feature along the top of the Crossing). A plausible uncertainty of the PA of $\pm 1^{\circ}$ would correspond to an uncertainty in decl. of $\pm 1.{''}8$ in the Crossing, thus allowing an alignment of the HH 269 axis with any of the three compact sources. At a greater distance the alignment passes close to AC Ori.

5.1.1. mm 9 and an Associated N_2H^+ clump

mm 9 is located in the NW portion of the elliptical region defining the shocks associated with the Crossing-Group. It is located slightly offset within the Crossing-Group but along the axis of the HH 269 flow if that axis has the allowable error of 1°. It was measured at 3 mm as a $>5\sigma$ detection by Eisner & Carpenter (2006), who note that it has no near-infrared counterpart.

In addition, mm 9 lies within Core 2 found by Teng & Hirano (2020) in their 5" resolution map in N_2H^+ emission in the J=3-2 line along a north-south feature within the background Orion Molecular Cloud. Two of the Teng & Hirano (2020) cores are shown in Figure 1. The heliocentric velocity of Core 2 is about 24.6 km s⁻¹. More recently, Hacar et al. (2020) mapped the same region with 10" resolution in the N_2H^+ J=7-6 transition, an emission-line selectively coming from very high-density gas $n(H_2) > 10^7$ cm⁻³. In that study, the authors established a strong correlation of high-density N_2H^+ knots and very young stars, which argues that this region contains a potential source of the material causing the HH 269 shocks. Although Teng & Hirano (2020) argued that the Core 2 lies in the background Orion Molecular Cloud, Hacar et al. (2020) place it within the Orion-S Cloud.

5.1.2. DRS 1186

DRS 1186 lies closest to the HH 269 axis of 275°. Little is known about it, although the discovery paper (Zapata et al. 2004) shows the source to have a microjet of about 0."5 extending to the NW, not at all close to the axis of the HH 269 features. This makes it an unlikely source. Nearby there is a west-oriented shock at 5:35:14.3–5:23:51 with $V_{\text{tan,[N II]}}$ = 8 km s⁻¹ but is at the limit of detectability. The position of the shock gives no support for association of DRS 1186 with HH 269.

5.1.3. COUP 632

COUP 632 lies on the northern boundary of the axis of HH 269. Appendix A9 of Rivilla et al. (2013) summarizes well the characteristics of COUP 632, although they incorrectly assign it as the source of HH 529 (O'Dell et al. 2015). It is seen in X-rays, through the infrared, and in short-wavelength radio radiation.

COUP 632 was identified in O'Dell et al. (2015) as the source of the HH 1132 east-jet that emerges with PA = 107° from within the Orion-S Cloud at the position shown with a square in Figures 1 and 2. The emergence position is quite obvious in time-sequence F656N H α images (O'Dell et al. 2015) rendered as a movie. The axis of this east-jet points exactly at COUP 632 with an opening-COUP 632 separation of 6.75.

This means that COUP 632 is the likely source of one collimated outflow (HH 1132 east-jet), but linking it to HH 269 requires that another jet be pointed toward $PA = 275^{\circ}$. A bipolar system would require the west-jet to be pointed toward

 $PA=287^{\circ}.$ A compounding problem to association of the HH 1132 east-jet and the HH 269 shocks is that both are blueshifted. The east-moving HH 1132 moves at a spatial velocity of 116 km s $^{-1}$ with $\Theta=32^{\circ}(O'Dell$ et al. 2015) while the Crossing-Group shocks have $PA=275^{\circ},~\Theta=59\pm10^{\circ},$ and space velocity 67 ± 12 km s $^{-1}.$

A strong selection effect exists for finding blueshifted components in the Huygens Region because the redshifted component would be headed toward the MIF and disappearance behind the PDR. Likewise, a redshifted jet originating behind the PDR will not emerge into the low-extinction ionized gas. In a summary of outflows, O'Dell et al. (2015) finds 27 mono-polar flows (all blueshifted), 8 bipolar flows (none with a well established redshift), and 7 multi-polar flows (all blueshifted). Therefore, there is plenty of evidence for nonbipolar flows in the Huygens Region and COUP 632 may be such a source.

If COUP 632 is the source, then it lies within the Orion-S Cloud. The separation of the Crossing-Group of moving features from COUP 632 is $10\rlap.{''}1$ (0.0188 pc). Adopting that object as the source and using $\Theta=59^\circ$ puts COUP 632 (0.031 pc) beyond the plane containing the Crossing-Group shocks. The separation in the plane of the sky of the Crossing-Group shocks and the SE-NW transition established in Paper II is $23\rlap.{''}$ (0.0427 pc). This means that COUP 632 is still within the Cloud. If it is also the source of the HH 1132 east-jet, then this interpretation is fully consistent with the break-out of that feature.

6. Two Series of Shocks Within the Crossing that are Not Related to HH 269

There are large-scale shocks of note falling within the Crossing that have no relation to HH 269. In the tangential velocities study of O'Dell et al. (2015) using HST WFC3 and WFPC2 images, a series of concentric strongly curved arcs was found in [O III] motions images in the Crossing, as shown in Figure 11 of that paper. These lie between mm 9 and the Dark Arc and were attributed to outflow from an undetected source a few arcseconds north of mm 9. We show in Figure 3 that these features are also seen in the superior WFC3 [O III] images adjusted in brightness and contrast to best display this area. We now see that they are not a circular motion away from an empty position designated as the Blank-West in O'Dell et al. (2015), but are instead the lead features in a series of bow-shock shapes driven by a more distant source to the SSW. At 7."5 west of their crests, a series of three partial shocks is also seen. Their more northerly orientation indicates a different source than that producing the former group of bow shocks. If they do have the same source, their axes intersect well south of the Crossing.

7. Most of the HH 269 Components are Formed from Episodic Outflows

The series of well-defined bow shocks that we see in the Middle-Group, East, and West components argue in favor of the driving jet being episodic because each period of flow would produce a single shock or a set of tightly grouped shocks. The $V_{\rm tan}$ and separations of the four main components indicate the time intervals between outflows: Crossing-Group and Middle-Group, 1900 yr; Middle-Group and East, 2500 yr; and East and West, 2600 yr. These time intervals are similar to

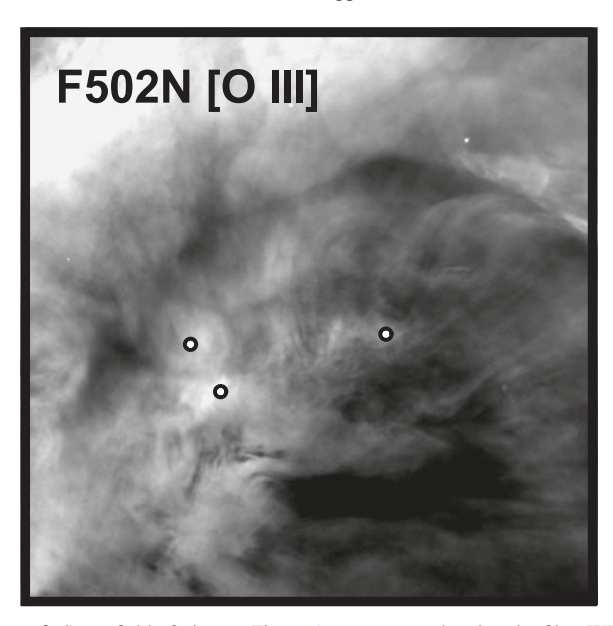


Figure 3. Same field of view as Figure 1 except now showing the filter WFC3 F502N [O III] image. The display is adjusted to best show the faint arcs north of source mm 9 but inside the Dark Arc. Their motions were reported in O'Dell et al. (2015).

those found in other outflows in the Huygens Region (O'Dell & Henney 2008).

The HH 269 Crossing-Group component lacks the well-defined bow shocks seen in the Middle-Group, East, and West components. This is consistent with this component not representing a single outflow, but rather a submerged outflow passing through the near side of the Orion-S Cloud.

8. Discussion and Conclusions

In Paper III we established that the Crossing is centered on a local rise in the nearer side of the Orion-S Cloud, which then flattens to the SW. Now we see that the Crossing-Group, the first visual components of HH 269, appears there. This suggests that a change in the local topography has determined where the flow producing the Crossing-Group breaks out.

This conclusion is reinforced by the fact that the E-W line along which the HH 269 features appear is also where the [O III] emission changes from domination by a component clearly near the MIF to lower velocity components associated with the NIL, a behavior that extends to the SW.

- Taken together, these points mean that the structure of the nearer ionized layer of the Orion-S Cloud influences where one can see the results of the HH 269 flow, and this flow does not influence the structure.
- 2. Two young stars are candidate sources of the collimated outflow that drives HH 269-the mm 9 source associated with N_2H^+ Clump 2 and the nearby COUP 632.
- 3. At 10."1 the obscured star COUP 632 has all the properties of a young star that produces jets; it has already been identified as the source of HH 1132, which is moving toward 108° or slightly less (O'Dell et al. 2015).

The reciprocal of its motion is 288°, producing a poor match to the PA of HH269 of 275° \pm 1°. More troubling is that both HH 1132 and HH 269 are clearly blueshifted ($V_{\rm r,[N\ II]}=-40~{\rm km\ s}^{-1}$ (O'Dell et al. 2015) and $-14\pm5~{\rm km\ s}^{-1}$, respectively). However, multi-polar outflows in the Huygens have been found (O'Dell et al. 2015). If this is the source, it lies in the western portion of the Orion-S Cloud.

- 4. mm 9 is located within the high-density N₂H⁺ Clump 2, which is a likely source of new star formation, and must lie close to the surface of the ionized layer of the Orion-S Cloud that faces the observer. Given its high extinction, it is likely to be within or beyond the underlying PDR.
- 5. The spatial separations and velocities of the components of HH 269 suggest that these are the result of intermittent jet activity at intervals of about 1900–2600 yr.

The observational data were obtained from observations with the NASA/ESA Hubble Space Telescope, obtained at the Space Telescope Science Institute (GO 12543), which is operated by the Association of Universities for Research in Astronomy, Inc., under NASA Contract No. NAS 5-26555; the Kitt Peak National Observatory and the Cerro Tololo Interamerican Observatory operated by the Association of Universities for Research in Astronomy, Inc., under cooperative agreement with the National Science Foundation; and the San Pedro Mártir Observatory operated by the Universidad Nacional Autónoma de México. We have made extensive use of the SIMBAD database, operated at CDS, Strasbourg, France and its mirror site at Harvard University, and to NASA's Astrophysics Data System Bibliographic Services. GJF acknowledges support by NSF (1816537, 1910687), NASA (ATP 17-ATP17-0141), and STScI (HST-AR- 15018).

ORCID iDs

```
C. R. O'Dell https://orcid.org/0000-0003-3323-2310
N. P. Abel https://orcid.org/0000-0003-1791-723X
G. J. Ferland https://orcid.org/0000-0003-4503-6333
```

References

```
Bally, J., O'Dell, C. R., & McCaughrean, M. J. 2000, AJ, 119, 2119
Da Rio, N., Robberto, M., Soderblom, D. R., et al. 2009, ApJS, 183, 261
Eisner, J. A., & Carpenter, J. M. 2006, ApJ, 641, 1162
García-Díaz, Ma.-T., Henney, W. J., López, J. A., & Doi, T. 2008, RMxAA,
Getman, K. V., Feigelson, E. D., Grosso, N., et al. 2005, ApJS, 160, 353
Hacar, A., Hogerheijde, M. R., Harsono, D., et al. 2020, A&A, 644, A133
Kounkel, M., Hartmann, L., Loinard, L., et al. 2017, ApJ, 834, 142
O'Dell, C. R., Abel, N. P., & Ferland, G. J. 2020, ApJ, 891, 46
O'Dell, C. R., Abel, N. P., & Ferland, G. J. 2021a, ApJ, 907, 119
O'Dell, C. R., Abel, N. P., & Ferland, G. J. 2021b, ApJ, 908, 162
O'Dell, C. R., Ferland, G. J., Henney, W. J., et al. 2015, AJ, 150, 108
O'Dell, C. R., & Henney, W. J. 2008, AJ, 136, 1566
Rivilla, V. M., Martín-Pintado, J., Sanz-Forcada, J., et al. 2013, MNRAS,
  434, 2313
Stanke, T., McCaughrean, M. J., & Zinneker, H. 2002, A&A, 392, 239
Teng, Y.-H., & Hirano, N. 2020, ApJ, 893, 63
Walter, D. K., O'Dell, C. R., Hu, X., et al. 1995, PASP, 107, 686
Zapata, L. A., Rodríguez, L. F., Kurtz, S. E., et al. 2004, ApJL, 610, L121
```